Available online at www.sciencedirect.com
ScienceDirect
Physics Procedia 3 (2010) 1411–1416
Physics Procedia
www.elsevier.com/locate/procedia

How local factors affect the exponents of forced polymer translocation through a nano-pore

Aniket Bhattacharya[a]

[a]Department of Physics, University of Central Florida, Orlando, Florida 32816, USA.

We study polymer translocation through a narrow pore driven by a bias present inside the pore with an aim to compare predictions of the existing theoretical results with those that we obtain using Langevin dynamics simulation in three dimensions(3D). We find that the translocation exponent α ($\langle\tau\rangle \sim N^{\alpha}$) decreases from 1.35 to 1.2 as the width of the pore is decreased from 1.5σ to 1.1σ. The exponent $\alpha = 1.2$ (extracted from chain lengths up to N = 256) not only violates the lower limit $1+\nu$ proposed by Kantor and Kardar (Y. Kantor and M. Kardar, Phys. Rev. E, **69**, 021806 (2004)) earlier but also lower than the more recently proposed lower limit $(1+2\nu)/(1+\nu)$ by Vocks *et al.* (H. Vocks, D. Panja, G. T. Barkema, and R. C. Ball, *J. Phys.: Condens. Matter* **20**, 095224 (2008)). We find that the average $\langle\bar{R}_g\rangle$ calculated during the entire translocation process is dominated by the equilibrium configurations at the *cis* side and therefore, relatively insensitive to the pore width and approximately described by the equilibrium Flory exponent ν. The velocity of the center of mass of the translocating chain on the contrary exhibits a systematic variation. Therefore, if we assume ($\langle\tau\rangle \sim \langle\bar{R}_g\rangle/\langle v_{CM}\rangle$, the dependence of $\langle v_{CM}\rangle$ on the pore width appears to be the primary factor that affects the translocation exponent.

1. INTRODUCTION

It has been demonstrated experimentally[1,2] that when a DNA passes through a nanopore subject to a bias across the pore, the histogram of the mean first passage times(MFPT) contains characteristics of the translocated DNA that shows prospects to design a fast and cheap sequence detection device. Since then the study of polymer translocation through a small pore has remained an active field of study[4]-[21]. The prospect of nano-pore based sequence detection methods has been investigated using computer simulation studies. It has been found that the *residence time* of the individual building blocks of a heteropolymer shows novel interference pattern containing detailed information about the sequence that has translocated through the pore[17].

The mean translocation time and the residence time will be a function of the specific sequence of an individual chain. However, the scaling and universal aspects of the translocation process can be conveniently studied using a model homopolymer. Despite its simplicity, several aspects of the homopolymer translocation are still intriguing with unresolved issues. While the case of an unbiased translocation is more transparent, simulation studies for driven translocation do not support theoretical results obtained using

doi:10.1016/j.phpro.2010.01.200

simple scaling arguments[8,9,12]. For the case of forced translocation Kantor and Kardar[8] assumed

$$\langle \tau \rangle \sim \langle R_g \rangle / \langle v_{CM} \rangle \ . \tag{1}$$

Further, if one assumes $R_g \sim N^{\nu}$ and $v_{CM} \sim 1/N$, as originally proposed by Kantor and Kardar[8], one gets $\langle \tau \rangle \sim N^{1+\nu}$. Kantor and Kardar argued that that since the chain is only driven at one point inside the narrow pore, the accompanying change in its shape due to the bias is insignificant for the rest of the chain and therefore, the chain in this case is also described by the equilibrium Flory exponent ν. They also assumed (as in the case of unbiased translocation) that the result $v_{CM} \sim 1/N$ is still valid in presence of a wall with a narrow pore. While this estimate is appealing at a first glance, repeated numerical studies (including their own numerical studies) using several different methods have failed to verify it. Kantor and Kardar reported $\alpha = 1.5 < 1 + \nu = 1.75$ from Lattice MC simulation of self-avoiding chains in $2D$. They argued that finite size effects are severe in this case and the relation $\langle \tau \rangle \sim N^{1+\nu}$ should be taken as an lower bound that will be seen only for the extremely large chains. Vocks *et al.* on the contrary, using arguments about memory effects in the monomer dynamics came up with an alternate estimate[12] $\langle \tau \rangle \sim N^{\frac{1+2\nu}{1+\nu}}$ in 3D.

Here we provide a brief summary and analysis of how the translocation exponent α is altered as one decreases the pore diameter w_p. We find that the exponent α decreases systematically as one decreases the pore diameter w_p. We further observe that despite significant shape changes that occur during the translocation, the dynamics is still dominated by the equilibrium configuration at the *cis* side, and therefore, the chain is still described by the equilibrium Flory exponent. The velocity of the center of mass does not scale as $1/N$, but the exponent δ ($\langle v_{CM} \rangle \sim 1/N^{\delta}$) decreases monotonically as the pore diameter is decreased. Our simulation studies further reveal that the chain is out of equilibrium as evident from very different chain conformations and their evolution at the *cis* and the *trans* side during the translocation process.

2. THE MODEL

We have used the "Kremer-Grest" bead spring model to mimic a strand of DNA [22]. Excluded volume interaction between monomers is modeled by a short range repulsive LJ potential

$$\begin{aligned} U_{LJ}(r) &= 4\epsilon[(\frac{\sigma}{r})^{12} - (\frac{\sigma}{r})^{6}] + \epsilon \text{ for } \ r \leq 2^{1/6}\sigma \\ &= 0 \text{ for } \ r > 2^{1/6}\sigma \ . \end{aligned}$$

Here, σ is the diameter of a monomer, and ϵ is the strength of the potential. The connectivity between neighboring monomers is modeled as a Finite Extension Nonlinear Elastic (FENE) spring with $U_{FENE}(r) = -\frac{1}{2}kR_0^2 \ln(1 - r^2/R_0^2)$, where r is the distance between consecutive monomers, k is the spring constant and R_0 is the maximum allowed separation between connected monomers. We use the Langevin dynamics with the equation of motion $\ddot{\vec{r}}_i = -\vec{\nabla} U_i - \Gamma \dot{\vec{r}}_i + \vec{W}_i(t)$. Here Γ is the monomer friction coefficient and $\vec{W}_i(t)$, is

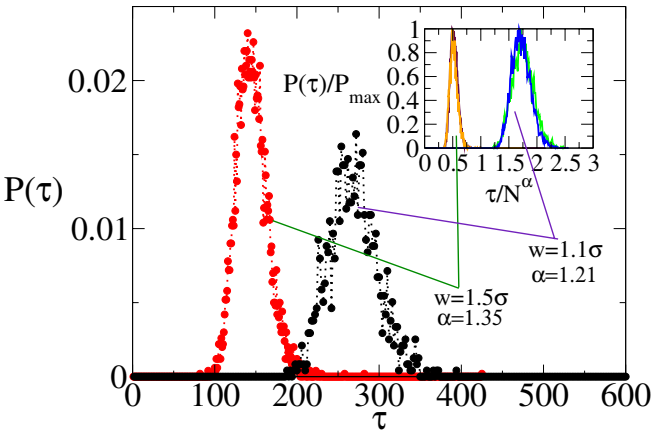

Figure 1. Histogram $P(\tau)$ of flight times for pore diameters 1.1σ (black) and 1.5σ (red) for chain length $N = 64$. The inset shows the corresponding data collapse for N=64 and N=128 where the τ-axis has been scaled by $1/N^{\alpha}$ and the y-axis has been scaled by the maximum value of the histogram.

a Gaussian white noise with zero mean at a temperature T, and satisfies the fluctuation-dissipation relation: $< \vec{W}_i(t) \cdot \vec{W}_j(t') >= 6k_BT\Gamma\,\delta_{ij}\,\delta(t-t')$. The purely repulsive wall consists of one monolayer of LJ particles on a *triangular lattice* at the xy plane at $z = 0$. The pore is created by removing the particle at the center. In this article to address the effects arising due to the finite width of the pore, we have considered wall particles with Lennard-Jones diameter form 1.1σ - 1.5σ. Inside the pore, the polymer beads experience a constant force F and a repulsive potential from the inside wall of the pore. The reduced units of length, time and temperature are chosen to be σ, $\sigma\sqrt{\frac{m}{\epsilon}}$, and ϵ/k_B respectively. For the spring potential we have chosen $k = 30$ and $R_{ij} = 1.5\sigma$, the friction co-efficient $\Gamma = 1.0$, and the temperature is kept at $1.5/k_B$ throughout the simulation.

We carried out simulations for chain lengths N from $16 - 256$ for with a biasing force $F = 6$. Initially the first monomer of the chain is placed at the entry of the pore. Keeping the first monomer in its original position the rest of the chain is then equilibrating for times at least an amount proportional to the $N^{1+2\nu}$. The chain is then allowed to move through the pore driven by the field present inside the pore. When the last monomer exits the pore we stop the simulation and note the translocation time and then repeat the same for 5000 such trials.

3. RESULTS

Fig. 1 shows the histogram of for the mean first passage times (MFPT) for two different values of the pore width ($w_p = 1.1\sigma$ and 1.5σ). For smaller pore diameters the local barriers increase the average translocation time. Therefore, one would like to know how this affects the chain length dependence of the translocation process. This is clearly manifested at the inset of Fig. 1 where the normalized histograms for MFPT are shown

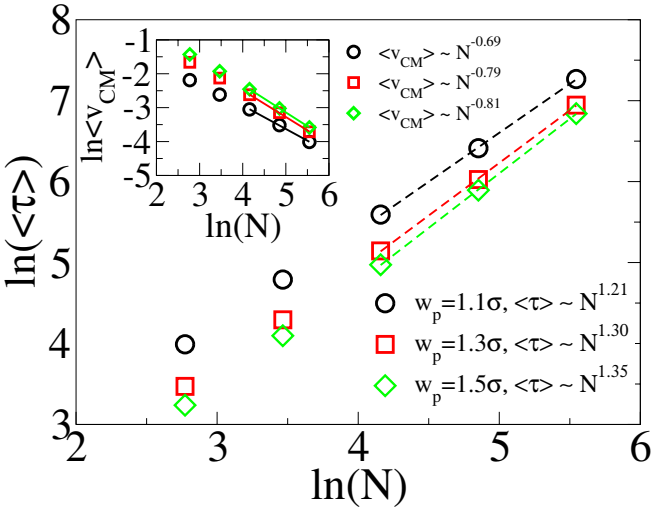

Figure 2. Scaling of the mean translocation time $\langle\tau\rangle$ (logarithmic scale) as a function of chain length N (logarithmic scale) for three different values of the pore diameter w_p. The inset shows corresponding scaling plots for the v_{CM}. The black circles, red squares, and green diamonds correspond to $w_p = 1.1\sigma$, 1.3σ, 1.5σ respectively. Lines through the points correspond to linear regression fits using last three points in each case.

for N=64 and N=128 for pore width 1.1σ and 1.5σ respectively. To demonstrate the pore width dependence of the τ-exponent ($N \sim \tau^{\alpha}$), we scale the time axis is by N^{α}. We find that two different values of α are needed ($\alpha = 1.21$ for and $w_p = 1.1\sigma$ and $\alpha = 1.35$ for and $w_p = 1.5\sigma$) for the scaled histograms. This is consistent with Fig. 2 where we extract the translocation exponent α from the slope of the average translocation time as a function of chain length for several values of the pore diameter w_p. We find that the exponent α systematically decreases as a function of the pore width from 1.36 to 1.21 for the chain lengths considered here. The inset shows the corresponding variation of the velocity of the center of mass of the chain and we find that exponent δ ($v_{CM} \sim 1/N^{\delta}$) decreases from 0.81 to 0.69.

During the translocation process we have monitored several aspects of the shape variation of the chain. Fig. 3 shows the variation of $\bar{R}_g$ (we use the notation $\bar{R}_g$ for the radius of gyration of the translocating chain) as a function of N for different pore diameters. On the same plot we have shown the variation of the equilibrium radius of gyration R_g for a chain clamped at the center of the pore. We notice that the translocating chain is approximately described by the equilibrium Flory exponent $\langle\bar{R}_g\rangle \sim N^{0.6}$ despite the fact the chain undergoes significant shape changes (top inset). We notice that the chain extension is maximum when it is almost half way through the pore. We have further extended the analysis by looking at the gyration radii both on the *trans* side ($R_g^{trans}(m)$) and the *cis* side ($R_g^{cis}(N-m)$) separately as a function of the translocated segments m (Fig. 3(lower inset)). One immediately notices that the dependence of $R_g^{trans}(m)$ and $R_g^{cis}(m)$ as a

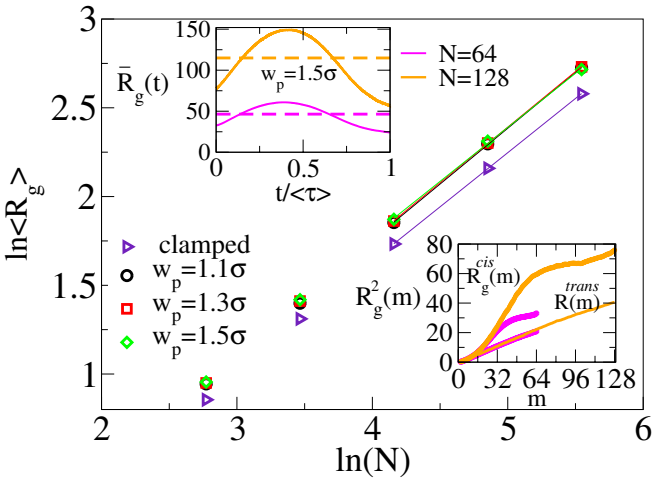

Figure 3. Scaling of radius of gyration of the translocating chain $\langle \bar{R}_g \rangle$ as well as equilibrium radius of gyration R_g of a clamped chain ((logarithmic scale) as a function of chain length N (logarithmic scale) for three different values of pore width. Purple triangles refer to the clamped chain and other symbols have the same meaning as in Fig. 2

function of the chain segment m reveal very different characteristics. Theoretical models need to take into account this basic asymmetry in *cis* and *trans* conformations of the translocating chain.

4. SUMMARY & DISCUSSION

To summarize, we have used Langevin dynamics in 3D to study how the pore geometry affects the translocation exponent of a driven translocating chain through a nanopore. We find that a smaller pore reduces the value of the translocation exponent. We further notice that the chain undergoes a significant shape change during the fast translocation process, contrary to what assumed by Kantor and Kardar formulating the theory of forced translocation. However, despite significant distortion, a careful observation reveals that the average $\langle R_g \rangle$ is *still dominated by its equilibrium value at the beginning of the translocation process* and hence the chain is still described by the equilibrium Flory exponent. We further observe that the chain conformations at the *cis* and *trans* sides are very different and clearly reveal out of equilibrium characteristics. Therefore, in the theoretical description of the forced translocation problem one needs to introduce additional slow variables (such as gyration radii at the *cis* and *trans* compartment) along with the s-coordinate to accommodate these features. A more detailed account of these studies will be reported elsewhere[23].

5. ACKNOWLEDGEMENT

I am indebted to Prof. Tapio Ala-Nissila and Prof. Kurt Binder for many valuable discussions on various aspects of the translocation problem.

REFERENCES

1. J. J. Kasianowitch, E. Brandin, D. Branton, and D. Deamer, Proc. Natl. Acad. Sci. U.S.A. **93**, 13770 (1996); A. Meller, L. Nivon, E. Brandin, J. Golovchenko, and D. Branton, *ibid* **97**, 1097 (2000).
2. J. L. Li, M. Gershow, D. Stein, E. Brandin, and J. A. Golovchenko, Nat. Mater. **2**, 611 (2003); A. J. Storm, J. H. Chen, X. S. Ling, H. W. Zandbergen, and C. Dekker, *ibid* **2**, 537 (2003).
3. B. Alberts *et al., Molecular Biology of the Cell* (Garland Publishing, New York, 1994).
4. W. Sung and P. J. Park, Phys. Rev. Lett. **77**, 783 (1996).
5. M. Muthukumar, J. Chem. Phys. **111**, 10371 (1999).
6. D. K. Lubensky and D. Nelson, Biophys. J. **77**, 1824 (1999).
7. J. Chuang, Y. Kantor, and M. Kardar, Phys. Rev. E, **65**, 011802 (2001).
8. Y. Kantor and M. Kardar, Phys. Rev. E, **69**, 021806 (2004).
9. J. L. A. Dubbledam, A. Milchev, V. G. Rostiashvili, and T. Vilgis, Phys. Rev. E **76**, 010801(R) (2007); J. L. A. Dubbledam, A. Milchev, V. G. Rostiashvili, and T. Vilgis, Europhysics Letters **79** 18002 (2007).
10. J. K. Wolterink, G. T. Barkema, and D. Panja, *Phys. Rev. Lett.* **96**, 208301 (2006).
11. D. Panja, G. T. Barkema, and R. C. Ball, *J. Phys.: Condens. Matter* **19**, 432202 (2007); *ibid***20**, 075101 (2008).
12. H. Vocks, D. Panja, G. T. Barkema, and R. C. Ball, *J. Phys.: Condens. Matter***20**, 095224 (2008).
13. A. Milchev, K. Binder, and A. Bhattacharya, J. Chem. Phys. **121**, 6042 (2004).
14. K. Luo, T. Ala-Nissila, and S-C. Ying, J. Chem. Phys. **124**, 034714 (2006). *ibid***124**, 114704 (2006);
15. I. Huopaniemi, K. Luo, T. Ala-Nissila, S-C. Ying, J. Chem. Phys. **125**, 124901 (2006).
16. D. Wei, W. Yang, X. Jin, and Q. Liao, J. Chem. Phys. **126**, 204901 (2007)
17. K. Luo, T. Ala-Nissila, and S-C. Ying, and Aniket Bhattacharya J. Chem. Phys. **126** 145101 (2006); Phys. Rev. Lett. **99** 148102 (2007); *ibid* **100** 058101 (2008).
18. S. Matysiak, A. Montesi, M. Pasquali, A. . Kolomeisky, C. Clementi, Phys. Rev. Lett. **96** 118103 (2006).
19. M. G. Gauthier and G. W. Slater, Eur. Phys. J. E **25**, 17 (2008).
20. K. Luo, S. Ollila, I. Huopaniemi, T. Ala-Nissila, P. Pomorski, M. Karttunen, S-C. Ying, and A. Bhattacharya, Phys. Rev. E. **78** 050901(R) (2008); *ibid* **78**, 061911 (2008); *ibid* **78**, 061918 (2008).
21. A. Bhattacharya, W. Morrison, K. Luo, T. Ala-Nissila, S. C. Ying, A. Milchev, and K. Binder, Eur. Phys. J. E **29** 423 (2009).
22. G. S. Grest & K. Kremer, Phys. Rev. A *33*, 3628 (1986).
23. Aniket Bhattacharya and Kurt Binder (to be published).